An explicit analytical solution for sound propagation in a three-dimensional penetrable wedge with small apex angle[a)]

Pavel S. Petrov[b)]
V.I.Il'ichev Pacific Oceanological Institute, 43, Baltiyskaya Street, Vladivostok, 690041, Russia

Frédéric Sturm
Laboratoire de Mécanique des Fluides et d'Acoustique, Unité Mixte de Recherche, Centre National de la Recherche Scientifique 5509, Université de Lyon, École Centrale de Lyon, 36 Avenue Guy de Collongue, F-69134 Ecully Cedex, France

(Received 28 September 2015; revised 19 January 2016; accepted 24 February 2016; published online 25 March 2016)

A problem of sound propagation in a shallow-water waveguide with a weakly sloping penetrable bottom is considered. The adiabatic mode parabolic equations are used to approximate the solution of the three-dimensional (3D) Helmholtz equation by modal decomposition of the acoustic pressure field. The mode amplitudes satisfy parabolic equations that admit analytical solutions in the special case of the 3D wedge. Using the analytical formula for modal amplitudes, an explicit and remarkably simple expression for the acoustic pressure in the wedge is obtained. The proposed solution is validated by the comparison with a solution of the 3D penetrable wedge problem obtained using a fully 3D parabolic equation that includes a leading-order cross term correction.
 [http://dx.doi.org/10.1121/1.4944692]

[BTH] Pages: 1343–1352

I. INTRODUCTION

The problem of sound propagation in a three-dimensional (3D) penetrable wedge is widely considered a most representative benchmark for 3D modeling methods in computational acoustics.[1–4] Although the formulation of this problem is very simple, its solution reveals many interesting features of 3D sound propagation, such as horizontal refraction, mode interaction,[1,4] second arrival of the pulse signal,[5] apex diffraction, etc.[6,7] Accurate simulation of all these effects requires many sophisticated mathematical methods to be used.[6,7]

In the past two decades the 3D wedge problem was used in many papers for the validation of various approaches to 3D propagation modeling.[1] An analytical solution to this problem was derived by Deane and Buckingham[8] in the form of a superposition of image sources. The contribution of each image was represented in terms of a Bessel function expansion inside a certain improper integral. The convergence of this series may be very slow when considering wedges with small apex angles α (the number of image sources required may be estimated as $2\pi/\alpha$, and the number of Bessel terms required also grows as α increases). In addition, in the case of a very small apex angle α, the environment turns into something very close to the Pekeris waveguide and, fully exploiting this fact, we should be able to obtain a very simple analytical solution. This is the primary goal of the present study.

The paper is organized as follows. First, the problem is presented in Sec. II. In Sec. III the solution to the 3D Helmholtz equation in the wedge-shaped two-layer waveguide is represented in the form of normal mode expansion.[1] Then the adiabatic mode parabolic equations (MPEs)[9–12] are used to obtain the modal amplitudes. It turns out that MPEs may be easily solved analytically in our case. Thus, in Sec. IV we obtain an explicit asymptotic solution (for small angles α) for the problem of propagation in the wedge. Our solution may be seen as the direct generalization of the standard Pekeris[1] normal mode solution for the slightly tilted bottom. In Sec. V, we compare our resulting formula with the solution obtained using a 3D parabolic equation (PE) based model that includes a leading-order cross term in its formulation that was developed and validated in previous work.[13] The 3D PE model is first briefly described. It is then shown that for the particular case of $\alpha = 0.5°$, the two solutions are in very good agreement up to a propagation distance of 8 km from the source. Notice that our solution based on modal decomposition completely neglects physical effects such as mode interaction[10] and diffraction by the wedge apex.[6] However, it takes into account horizontal refraction effects very accurately and allows to reveal/confirm the inaccuracy of the 3D PE computation when cross terms are neglected.[13] Section VI concludes the paper.

II. PROBLEM FORMULATION

We consider a shallow-water waveguide with a tilted bottom as shown in the Fig. 1. The sea surface and the

[a)]Portions of this work were presented in "Asymptotic solution for the problem of acoustic waves propagation in a penetrable truncated wedge," Proceedings of the International Conference Days on Diffraction 2013, Saint-Petersburg, Russia, May 2013, and in "Sound propagation in a 3D wedge: An explicit asymptotic solution for the case of very small opening angle," Proceedings of the 1st International Conference and Exhibition on Underwater Acoustics, Corfu, Greece, June 2013. The preliminary results were also reported at these conferences.

[b)]Also at: Far Eastern Federal University, 8 Suhanova St., Vladivostok, 690950, Russia. Electronic mail: petrov@poi.dvo.ru

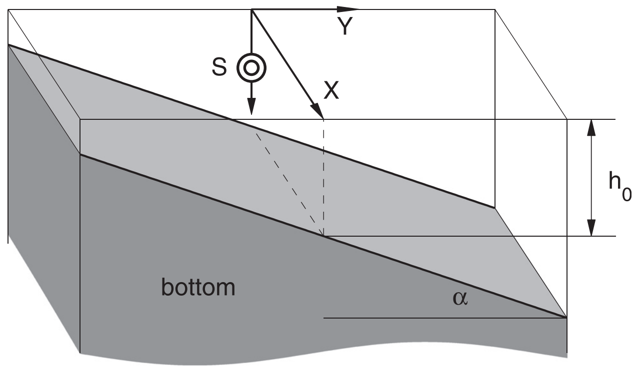

FIG. 1. A wedge-like waveguide with apex angle α and the x axis is aligned along the apex. The point source S is located at $x=0$, $y=0$, $z=z_s$.

bottom form a wedge with an apex angle denoted α. The sound speed and density in the lossless water column (upper layer) are denoted c_w and ρ_w, respectively, while the respective parameters in the halfspace bottom (lower layer) are denoted c_b and ρ_b, respectively. The attenuation in the bottom is denoted β_b. The z axis is directed downward (i.e., z is the depth), and the x,y are the horizontal Cartesian coordinates. In this coordinate system, the bottom relief is described by $\{z = h(y)\}$ with $h(y)$ defined by

$$h(y) = \begin{cases} h_0 + h_1(y) & \text{for } h_1(y) > -h_0 \\ 0, & \text{otherwise,} \end{cases} \tag{1}$$

where h_0 is a constant and $h_1(y)$ is given by

$$h_1(y) = \tan(\alpha) y. \tag{2}$$

A time-harmonic point source of frequency f is located in the water column at $x=0$, $y=0$, $z = z_s > 0$. The water depth at the source is thus equal to h_0 and is constant along the $\{y = 0\}$ direction.

We consider the problem of sound propagation in the wedge-like waveguide described above for the small apex angle α. The mathematical formulation is given in terms of the boundary problem in the domain $z \geq 0$ for the 3D Helmholtz equation for the sound pressure $P = P(x, y, z)$,

$$P_{xx} + P_{yy} + P_{zz} + \frac{\omega^2}{c^2}(1 + \mathrm{i}\eta\beta)^2 P = -\delta(x, y, z - z_s), \tag{3}$$

where $\omega = 2\pi f$ is the cyclic frequency, c and β denote, respectively, the sound speed and the attenuation expressed in dB per wavelength, both defined by their restrictions on each layer, and where $\eta = 1/(40\pi \log_{10} \mathrm{e})$. For instance, $c = c_w$ if $0 \leq z < h(y)$ and $c = c_b$ if $z > h(y)$. The 3D Helmholtz equation (3) is complemented with a pressure-release boundary condition at the sea surface $\{z = 0\}$,

$$P|_{z=0} = 0, \tag{4}$$

and the usual continuity conditions at the interface $\{z = h(y)\}$ for the sound pressure and the particle velocity

$$\begin{aligned} &P|_{z=h^-} = P|_{z=h^+}, \\ &\frac{1}{\rho_w}\frac{\partial P}{\partial \mathbf{n}}\bigg|_{z=h^-} = \frac{1}{\rho_b}\frac{\partial P}{\partial \mathbf{n}}\bigg|_{z=h^+}, \end{aligned} \tag{5}$$

where $\mathbf{n}$ denotes a unit normal vector to the interface $\{z = h(y)\}$ and the superscript notations "+" and "–" signify above and below the interface, respectively. We also assume that the standard radiation conditions are fulfilled at $R = \sqrt{x^2 + y^2 + z^2} \to \infty$. Note that for a rigorous formulation, it is also important to impose the so-called Meixner condition[6] in the neighbourhood of the apex (this condition ensures that the energy of the wave field is bounded in the neighbourhood of the wedge apex).

III. PROBLEM REDUCTION TO THE MPE

The adiabatic MPEs method was first developed by Collins,[9] and was later improved by Abawi *et al.*[10] to account for the mode interaction. An alternative approach to the MPE derivation from the Helmholtz equation was proposed by Trofimov[11] (see also Petrov *et al.*[12]). The derivations of MPE by Collins[9] and Trofimov[11] are drastically different. While the former is based on the operator square root approximation, the latter is accomplished using the method of multiple scales. The adiabatic MPE of Collins[9] may be converted into that of Trofimov[11] via the perturbative expansion of the mode wavenumbers with respect to the (small) bottom relief inhomogeneities magnitude.[1]

For the sake of completeness here, we briefly explain how to derive adiabatic MPE (in the form of Trofimov[11]) from the "horizontal" mode amplitude equations.[1,10] It was shown by Petrov and Petrova[14] that for small bottom inhomogeneities, i.e., $h_1 \ll h_0$, the solution of the elliptic boundary value problem based on the 3D Helmholtz equation may be approximated by the following truncated modal expansion:[27]

$$P(x, y, z) \approx \sum_{j=1}^{N_m} \mathcal{A}_j(x, y)\phi_j(z), \tag{6}$$

where $\phi_j(z)$ are the discrete spectrum eigenfunctions satisfying the following standard spectral problem[1] (only the first N_m modes are taken into account):

$$\begin{cases} \dfrac{\mathrm{d}^2\phi_j}{\mathrm{d}z^2} + \dfrac{\omega^2}{c^2}\phi_j = k_j^2\phi_j, \quad z \in]0, h_0[\cup]h_0, \infty[, \\ \phi_j|_{z=0} = 0, \\ \phi_j|_{z=h_0^-} = \phi_j|_{z=h_0^+}, \\ \dfrac{1}{\rho_w}\dfrac{\mathrm{d}\phi_j}{\mathrm{d}z}\bigg|_{z=h_0^-} = \dfrac{1}{\rho_b}\dfrac{\mathrm{d}\phi_j}{\mathrm{d}z}\bigg|_{z=h_0^+}, \\ \phi_j \to 0 \text{ as } z \to \infty. \end{cases} \tag{7}$$

Here, k_j^2, $1 \leq j \leq N_m$, denote the real-valued eigenvalues associated to the discrete eigenfunctions $\phi_j(z)$, $1 \leq j \leq N_m$, satisfying $k_1^2 > k_2^2 > \cdots > k_{N_m}^2$. The eigenfunctions $\phi_j(z)$, $1 \leq j \leq N_m$, satisfy also the orthonormality condition

$$\int_0^\infty \frac{\phi_\ell(z)\phi_j(z)}{\rho}\,\mathrm{d}z = \delta_{\ell j}, \tag{8}$$

where ρ denotes the density defined by its restrictions on each layer, and $\delta_{\ell j}$ denotes the Kronecker symbol (i.e., $\delta_{\ell j} = 1$ if $\ell = j$ and $\delta_{\ell j} = 0$ if $\ell \neq j$).

Let us turn now to the derivation of the system of coupled partial differential equations satisfied by the modal amplitudes $\mathcal{A}_j(x,y)$, $1 \le j \le N_m$. By first multiplying the Helmholtz equation (3) by $\phi_j(z)/\rho$, integrating in depth, then twice integrating by parts, and using the interface conditions at h_0 that have been transferred from the interface $\{z = h(y)\}$ to the horizontal plane $\{z = h_0\}$ [see Eq. (6) of Ref. 14], we obtain under the usual assumption $\eta\beta \ll 1$ the following equality:

$$\int_0^\infty \frac{1}{\rho}\left(P_{xx} + P_{yy} + k_j^2 P\right)\phi_j\,\mathrm{d}z + 2\mathrm{i}\eta\beta_b\frac{\omega^2}{c_b^2}\int_{h_0}^\infty \frac{P\phi_j}{\rho_b}\,\mathrm{d}z + h_1\left[\left(\frac{P_{zz}^+}{\rho_b} - \frac{P_{zz}^-}{\rho_w}\right)\phi_j(h_0) + \frac{1}{\rho_w}\frac{\mathrm{d}\phi_j}{\mathrm{d}z}(h_0^-)\left(P_z^- - P_z^+\right)\right] = -\delta(x)\delta(y)\frac{\phi_j(z_s)}{\rho_w}, \tag{9}$$

where $P_z^\pm = P_z|_{z=h_0^\pm}$ and $P_{zz}^\pm = P_{zz}|_{z=h_0^\pm}$. Introducing the modal expansion (6) in Eq. (9) and using the orthonormality condition (8) of the eigenfunctions $\phi_j(z)$, $1 \le j \le N_m$, we finally obtain the following system of coupled elliptic equations for the modal amplitudes $\mathcal{A}_j(x,y)$, $1 \le j \le N_m$:

$$\partial_x^2\mathcal{A}_j + \partial_y^2\mathcal{A}_j + k_j^2\mathcal{A}_j + \sum_{\ell=1}^{N_m}(h_1 B_{j\ell} + Q_{j\ell})\mathcal{A}_\ell = -\delta(x)\delta(y)\frac{\phi_j(z_s)}{\rho_w}, \tag{10}$$

where the coefficients of the coupling matrix[1] $B_{j\ell}$ and $Q_{j\ell}$ are given by

$$B_{j\ell} = \left(\frac{1}{\rho_b}\frac{\mathrm{d}^2\phi_\ell}{\mathrm{d}z^2}(h_0^+) - \frac{1}{\rho_w}\frac{\mathrm{d}^2\phi_\ell}{\mathrm{d}z^2}(h_0^-)\right)\phi_j(h_0) + \frac{1}{\rho_w}\frac{\mathrm{d}\phi_j}{\mathrm{d}z}(h_0^-)\left(\frac{\mathrm{d}\phi_\ell}{\mathrm{d}z}(h_0^-) - \frac{\mathrm{d}\phi_\ell}{\mathrm{d}z}(h_0^+)\right),$$

$$Q_{j\ell} = 2\mathrm{i}\eta\beta_b\frac{\omega^2}{c_b^2}\int_{h_0}^\infty \frac{\phi_\ell(z)\phi_j(z)}{\rho_b}\,\mathrm{d}z.$$

Notice that the integral $Q_{j\ell}$ is the sole term responsible for handling attenuation. Notice also that in the presence of a continuous spectrum (e.g., for the halfspace problem), parts of the sums in Eqs. (6) and (10) turn into integrals with respect to the spectral parameter. It is, however, clear from the rest of this section, that in the adiabatic case this is irrelevant (due to the adiabaticity assumption).

Now we make the standard adiabaticity assumption,[1,15,16] i.e., we assume that mode interaction in the system (10) is negligible, and we can therefore drop all non-diagonal terms $B_{j\ell}$ and $Q_{j\ell}$, $\ell \ne j$. This simplification usually works well in cases when the media parameters h_0, c_w, ρ_w, c_b, and ρ_b are chosen in such a way that f is not close to the cut-off frequency of a certain mode.[1] The uncoupled adiabatic approximation to the system (10) is written as

$$\partial_x^2\mathcal{A}_j + \partial_y^2\mathcal{A}_j + k_j^2\mathcal{A}_j + (h_1 B_{jj} + Q_{jj})\mathcal{A}_j = -\delta(x)\delta(y)\frac{\phi_j(z_s)}{\rho_w}, \tag{11}$$

where all equations may now be solved separately.

Finally, for each $1 \le j \le N_m$, near the x axis the solution of the (two-dimensional) 2D Helmholtz equation (11) may be approximated by the solution of the standard narrow-angle PE

$$2\mathrm{i}k_j\partial_x A_j + \partial_y^2 A_j + (h_1 B_{jj} + Q_{jj})A_j = 0, \tag{12}$$

whereas usually $A_j(x,y)$ is a slowly varying in x envelope function of the modal amplitude $\mathcal{A}_j(x,y)$ satisfying

$$\mathcal{A}_j(x,y) = \mathrm{e}^{\mathrm{i}k_j x}A_j(x,y)\,.$$

Note that the derivation of Eq. (12) is a standard procedure which can be found in many textbooks on wave propagation (see, e.g., Ref. 1). We set up the Cauchy problem for the MPEs (12) in the halfspace $\Omega_h = \{(x,y)\,|\,x \ge 0\}$ with the following Gaussian initial conditions designed to approximate the field produced by a point source

$$A_j(x,y)|_{x=0} = \bar{A}_j\,\mathrm{e}^{-k_j^2 y^2}, \tag{13}$$

where $\bar{A}_j = \phi_j(z_s)/(2\sqrt{\pi}\rho_w)$ (see Appendix B for the derivation of these expressions).

We emphasize again that the adiabatic MPE (12) is a slightly simplified version of the classical MPE of Collins.[9] More precisely, it is simply a linearization of the latter with respect to $h_1(y)$ (see Refs. 11 and 14). This linearization is clearly reasonable for small values of $h_1(y)$ in the domain of interest. In this form, Eq. (12) was first obtained by Trofimov[11] by means of the method of multiple scales.

We would like to stress again that there are two crucial assumptions in our approximation of the solution of Eq. (3) by the expansion

$$P(x,y,z) \approx \sum_{j=1}^{N_m} \mathrm{e}^{\mathrm{i}k_j x}A_j(x,y)\phi_j(z). \tag{14}$$

First, we neglect mode coupling [when turning Eq. (10) into Eq. (11)] and, second, we assume that propagation from the source at $x=0$, $y=0$ to the receiver at $x = x_r$, $y = 0$ is mostly paraxial [this fact is used in the transition from Eq. (11) to the MPEs (12)]. Clearly, both assumptions are valid for sufficiently small values of α, and therefore Eq. (14) is an asymptotic solution to the problem of sound propagation in the wedge. Since our main goal is the computation of the sound pressure in the water [i.e., for $0 \le z \le h(y)$], we may retain only the guided modes in the expansion (14), i.e., the modes corresponding to the discrete spectrum of Eq. (7).

IV. EXACT SOLUTION OF THE MPE FOR THE WEDGE CASE

A. Trapped modes in a two-layer waveguide

In the two-layer waveguide, the spectral problem (7) is of well-known Pekeris type.[1] The discrete spectrum wavenumbers k_j, $1 \le j \le N_m$, for such a problem can be determined from the dispersion relation (see, for instance, Ref. 17)

$$\tan(\kappa_{w,j}h_0)\rho_w\kappa_{b,j} + \rho_b\kappa_{w,j} = 0, \tag{15}$$

where $\kappa_{w,j} = (k_w^2 - k_j^2)^{1/2}$ and $\kappa_{b,j} = (k_j^2 - k_b^2)^{1/2}$ correspond to the vertical wavenumbers, respectively, in the water column and the bottom for the jth mode, with $k_w = \omega/c_w$ and $k_b = \omega/c_b$. The mode functions $\phi_j(z)$, $1 \le j \le N_m$, for the Pekeris waveguide are written as[1]

$$\phi_j(z) = \begin{cases} C_j^{-1}\sin(\kappa_{w,j}z) & \text{if } z \le h_0\,; \\ C_j^{-1}\sin(\kappa_{w,j}h_0)\mathrm{e}^{\kappa_{b,j}(h_0 - z)} & \text{if } z > h_0, \end{cases}$$

where C_j, $1 \le j \le N_m$, are normalization constants, introduced here so that $\int_0^{h_0}\phi_j^2(z)\rho_w^{-1}\,\mathrm{d}z + \int_{h_0}^{\infty}\phi_j^2(z)\rho_b^{-1}\,\mathrm{d}z = 1$, $1 \le j \le N_m$, and are given by

$$C_j = \left(\frac{h_0}{2\rho_w} - \frac{\sin(\kappa_{w,j}h_0)\cos(\kappa_{w,j}h_0)}{2\rho_w\kappa_{w,j}} + \frac{\sin^2(\kappa_{w,j}h_0)}{2\rho_b\kappa_{b,j}}\right)^{1/2}.$$

B. Formula for the amplitudes

For each $1 \le j \le N_m$, the MPE (12) may be rewritten as

$$2\mathrm{i}k_j\partial_x A_j + \partial_y^2 A_j + (b_j y + a_j)A_j = 0, \tag{16}$$

where $b_j = \tan(\alpha)B_{jj}$, with

$$B_{jj} = \left[\frac{k_w^2}{\rho_w} - \frac{k_b^2}{\rho_b} + k_j^2\left(\frac{1}{\rho_b} - \frac{1}{\rho_w}\right)\right]\frac{\sin^2(\kappa_{w,j}h_0)}{C_j^2} - (\rho_b - \rho_w)\frac{\kappa_{w,j}^2\cos^2(\kappa_{w,j}h_0)}{C_j^2\rho_w^2},$$

and where

$$a_j = 2\mathrm{i}\eta\beta_b k_b^2\int_{h_0}^{\infty}\frac{\phi_j^2(z)}{\rho_b}\,\mathrm{d}z = \frac{\mathrm{i}\eta\beta_b k_b^2}{\rho_b C_j^2\kappa_{b,j}}\sin^2(\kappa_{w,j}h_0) \tag{17}$$

is the modal attenuation coefficient for the jth mode (see Refs. 1 and 12 for more details).

The Cauchy problem for Eq. (16) admits an analytical solution, which may be written as

$$A_j(x,y) = \bar{A}_j\sqrt{\frac{1}{1+2\mathrm{i}k_j x}}\exp\left(-\frac{\left(yk_j - \frac{x^2 b_j}{4k_j}\right)^2}{1+2\mathrm{i}k_j x}\right) \times \exp\left(\frac{\mathrm{i}a_j x}{2k_j} + \frac{\mathrm{i}b_j yx}{2k_j} - \frac{\mathrm{i}x^3 b_j^2}{24k_j^3}\right). \tag{18}$$

Using the solutions (18) for $A_j(x,y)$ and the expansion equation (14), we may compute the acoustical pressure $P(x,y,z)$ and the respective transmission losses. Note that Eq. (18) reduces to the initial condition (13) at $x = 0$.

Although Eq. (16) is identical to the Schrödinger equation describing a particle in a constant force field (in a one-dimensional space), it cannot be found in standard textbooks on quantum mechanics, and it is difficult to figure out in which paper it was first derived. For instance, this result follows directly from the classical work of Wei and Norman,[18] and it is also written explicitly in a more general form in the paper by Prants.[19] For the sake of completeness, a derivation based on the Hausdorff formula is given in Appendix A (it follows Dattoli *et al.*[20] and Petrov[21] closely).

Note that formally $h_1(y)$ is not a linear function [as it follows from Eq. (1)] and we should assume it to be constant $h_1 = -h_0$ for

$$y < -h_0/\tan\alpha. \tag{19}$$

However, the adiabatic MPE approximation (14) itself is valid only inside a neighbourhood $\Omega_{\text{c.o.}}$ of the source where the bottom depth satisfies the inequalities

$$h_{\text{c.o.}}^m < h(y) < h_{\text{c.o.}}^{m+1},$$

where $h_{\text{c.o.}}^m = h_{\text{c.o.}}^m(f, c_w, c_b, \rho_w, \rho_b)$ denotes the cut-off depth of the mth guided mode (in particular, this inequality implies that our solution should not be used for the case when the source is located near the cut-off depth). Clearly, this inequality is much more restrictive than the condition (19), and we may consider the potential in Eq. (12) to be linear. We also point out that in wedge-like waveguide, the mode coupling effects outside $\Omega_{\text{c.o.}}$ may contribute to the field inside this domain due to horizontal refraction effects. Thus, we may expect formula (14) to be valid only inside a subdomain of $\Omega_{\text{c.o.}}$ for which this contribution is negligible. The comparisons presented in Sec. V B will show that all the approximations we made are reasonable and that the analytical solution (14) can be sufficiently accurate inside a relatively large domain.

We also note that our solution can be easily extended to the case when the y axis is not aligned along the wedge apex (i.e., to the case of a rotated coordinate system). The solution in Cartesian coordinates $\{x,y\}$, where the y axis is aligned at an angle θ to the isobath is derived and discussed in Appendix C.

V. NUMERICAL EXPERIMENTS

A. The 3D parabolic model with a leading-order cross term correction

We give here a brief description of the fully 3D wide-angle PE based model that we have used to compute a reference solution that naturally includes mode coupling effects. The 3D parabolic model under consideration here can be used to compute acoustic field in a multilayered waveguide composed of one water layer and one or several fluid sediment layers. The geometry of each layer is fully 3D. Cylindrical coordinates r,θ,z are used, where r and θ represent, respectively, the horizontal range and the azimuthal angle, both related to the Cartesian coordinates from Sec. II by $x = r\cos\theta$ and $y = r\sin\theta$, and z represents the depth, increasing downward. Considering a harmonic point source of frequency f, located at $r = 0$ and $z = z_s > 0$, and assuming

TABLE I. Horizontal wavenumbers for the normal modes of the discrete spectrum.

Mode no.	1	2	3	4
k_j	0.20724586	0.20030636	0.18771764	0.16819605

only outward propagation in range, the elliptic-type 3D Helmholtz equation is replaced by the following wide-angle 3D PE:

$$\partial_r \psi(r,\theta,z) = \mathrm{i}k_0 \left[\sum_{k=1}^{n_p} \frac{a_{k,n_p}\mathcal{X}}{\mathcal{I}+b_{k,n_p}\mathcal{X}} + \sum_{k=1}^{m_p} \frac{a_{k,m_p}\mathcal{Y}}{\mathcal{I}+b_{k,m_p}\mathcal{Y}} - \frac{1}{4}\mathcal{X}\mathcal{Y} \right] \psi(r,\theta,z), \qquad (20)$$

where the unknown $\psi(r,\theta,z)$ is the envelope function related to the acoustic pressure by $P(r,\theta,z) = H_0^{(1)}(k_0 r) \times \psi(r,\theta,z)$, with $H_0^{(1)}$ being the zeroth-order Hankel function of the first kind, and $k_0 = 2\pi f/c_0$ where c_0 is a reference sound speed (to be selected by the user). In Eq. (20), $\mathcal{I}$ denotes the identity operator, $\mathcal{X}$ is the 2D depth operator in the vertical rz-plane, and $\mathcal{Y}$ the azimuthal operator, defined as

$$\mathcal{X} = (n^2-1)\mathcal{I} + \frac{\rho}{k_0^2}\partial_z\left(\frac{1}{\rho}\partial_z\right), \quad \mathcal{Y} = \frac{1}{(k_0 r)^2}\partial_\theta^2,$$

where $n(r,\theta,z) = (c_0/c(r,\theta,z))(1+\mathrm{i}\eta\beta)$ denotes the complex (to account for lossy layers) index of refraction. As in Sec. II, c stands for the sound speed, β is the attenuation coefficient expressed in decibels per wavelength, while ρ denotes the density, constant within each layer. The accuracy of the solution $\psi(r,\theta,z)$ approximating the pressure field solution of the 3D Helmholtz equation can be controlled by selecting a sufficient number of Padé terms n_p and m_p, respectively, in depth and in azimuth. Note that the Padé coefficients in depth, a_{k,n_p}, b_{k,n_p}, $1 \le k \le n_p$, and in azimuth, a_{k,m_p}, b_{k,m_p}, $1 \le k \le m_p$, can be real or complex (to attenuate Gibb's oscillations; see, for instance, Refs. 22 and 23). Note also that the fully wide-angle capability of this 3D PE model is attributed to the presence of the last (cross-multiplied) operator $-(1/4)\mathcal{X}\mathcal{Y}$ appearing on the right-hand side of Eq. (20). From a practical point of view, this leading-order cross term operator has been incorporated (for more details, see Ref. 13) into an existing numerical code by adding a third step into the original two-step splitting based method of Ref. 4. The first step (hereafter, step 1) consists in

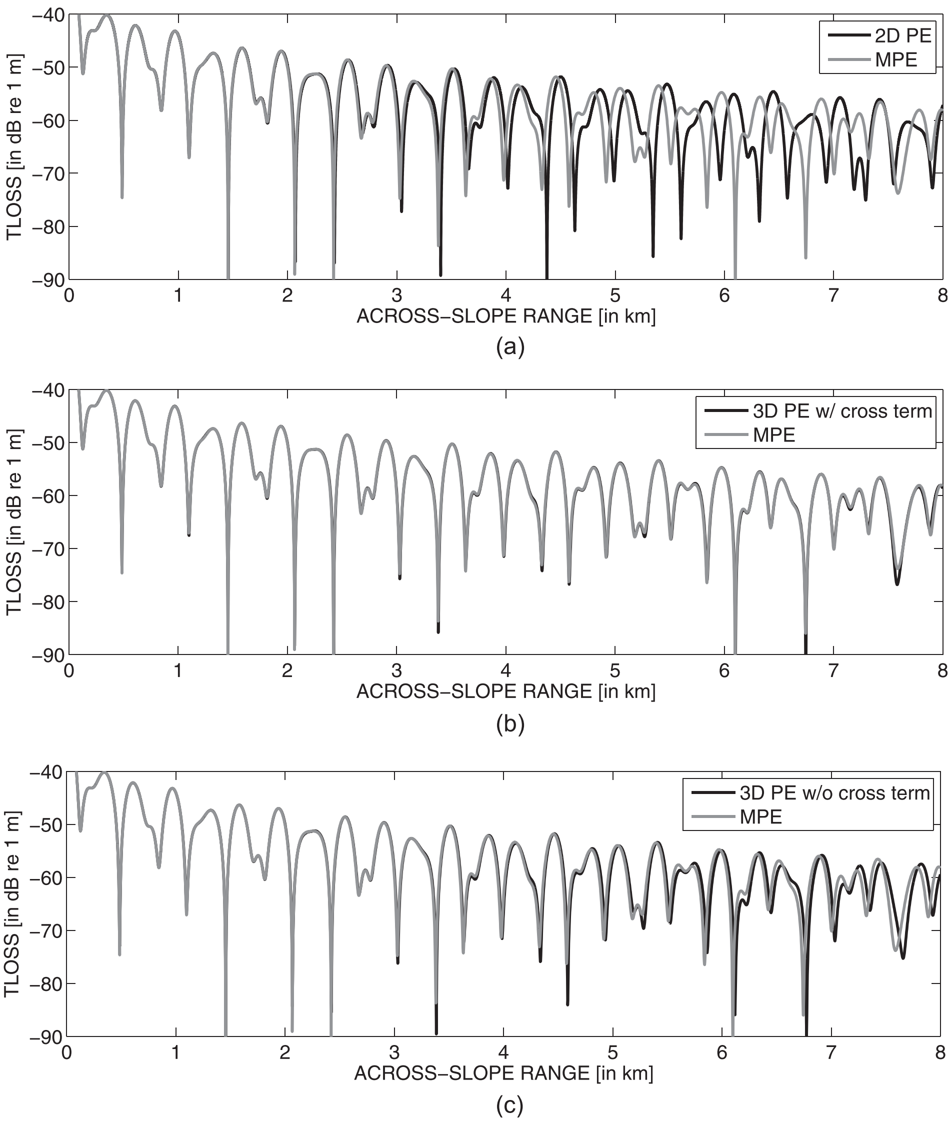

FIG. 2. Transmission loss (in dB re 1 m) curves at a receiver depth of 10 m in the across-slope direction corresponding to various PE solutions (black curves) and the same MPE solution (gray curves). The PE solutions correspond to one 2D computation (upper subplot) and two distinct 3D computations carried out, including (middle subplot) and ignoring (lower subplot) the leading-order cross correcting term (see discussion in Sec. V).

the evaluation of the exponential of the first sum on the right-hand side of Eq. (20), consisting of n_p rational-linear terms with operator $\mathcal{X}$. During step 2, the exponential of the second sum of m_p terms depending on $\mathcal{Y}$ in Eq. (20) is computed. The additional step 3 introduced in Ref. 13 is required to evaluate the exponential of the operator $-(1/4)\mathcal{X}\mathcal{Y}$. The three-step marching algorithm allows to compute $\psi(r_j+\Delta r,\theta,z)$ from the known function $\psi(r_j,\theta,z)$.

Note that the use of this 3D PE model as a reference model is justified by its previous validation on the 3D Acoustical Society of America (ASA) wedge test case.[13] In our case, the solution of 3D PE was also compared with the analytical solution of Deane and Buckingham,[8] and a very good agreement was observed. Additionally, our goal was to show that a very simple analytical solution proposed in this study can reveal an inaccuracy of the much more complicated 3D PE model (see the comparison in Sec. V B).

B. Numerical results

We consider a penetrable wedge-shaped waveguide with a slope angle α of 0.5°. We assume that the sound speed and the density in the water column are $c_w = 1500\,\mathrm{m/s}$ and $\rho_w = 1\,\mathrm{g/cm^3}$, while the respective parameters in the bottom are equal to $c_b = 2000\,\mathrm{m/s}$ and $\rho_b = 2\,\mathrm{g/cm^3}$. We also set the bottom depth at the source $\{y=0, x=0\}$ to $h_0 = 90\,\mathrm{m}$ (the source is located at a depth z_s of 10 m). The bottom attenuation is 0.5 dB per wavelength (the water layer is assumed to be lossless) and the source frequency is $f = 50\,\mathrm{Hz}$. In this waveguide, for a water depth of h_0, there are four trapped modes whose horizontal wavenumbers are given in Table I.

Both 2D and 3D PE computations presented hereafter were carried out using a range increment Δr of 2.5 m and a depth increment Δz of 0.25 m, and a reference sound speed value of 1500 m/s. The PE in-range marching algorithms were initialized at $r=0$ using a modal sum that includes only the propagating modes. The maximum computation range was 8 km. Note that the 2D PE solution was obtained by using only step 1 in the marching algorithm (i.e., retaining only the Padé sum containing the 2D depth operator $\mathcal{X}$). An eighth-order finite-difference azimuthal scheme with $M = 3240$ mesh points in azimuth was used in step 2. With the range r increasing, the number of azimuthal points was also increased in such a way that the arc length increments $\Delta s = r\Delta\theta$ remain $<\lambda/6$.

We display in Fig. 2 transmission loss-versus-range curves at a constant depth of 10 m and along the across-slope direction $\{y=0\}$, corresponding to a wide-angle 2D PE numerical solution ($n_p = 2$) and to two distinct wide-angle 3D PE numerical solutions ($n_p = 3,\ m_p = 1$) obtained with and

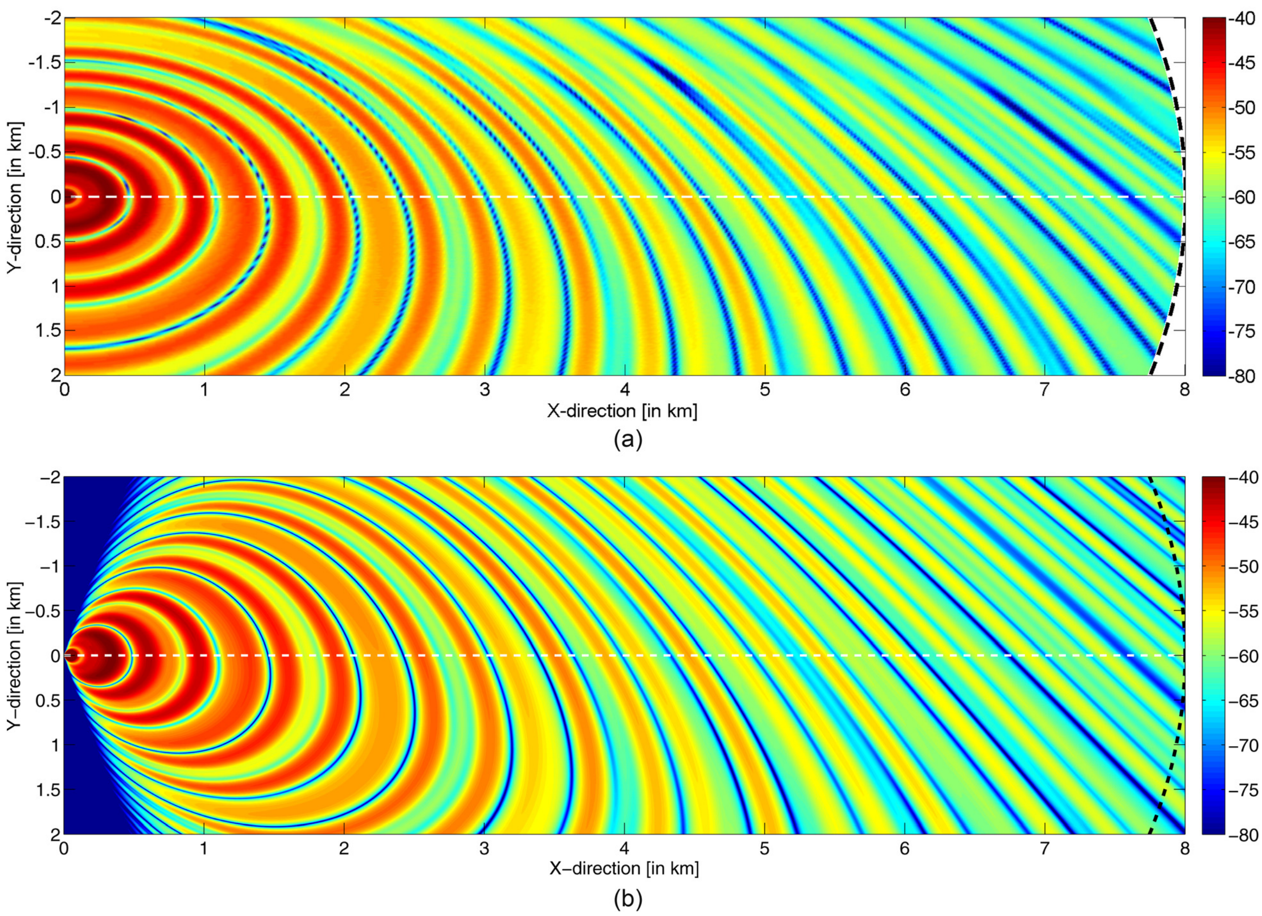

FIG. 3. (Color online) Transmission loss (horizontal slices at a receiver depth of 10 m) corresponding to 3D PE solution (upper subplot) and MPE solution (lower subplot). On each subplot, the 90 m isobath is indicated by a white dashed line.

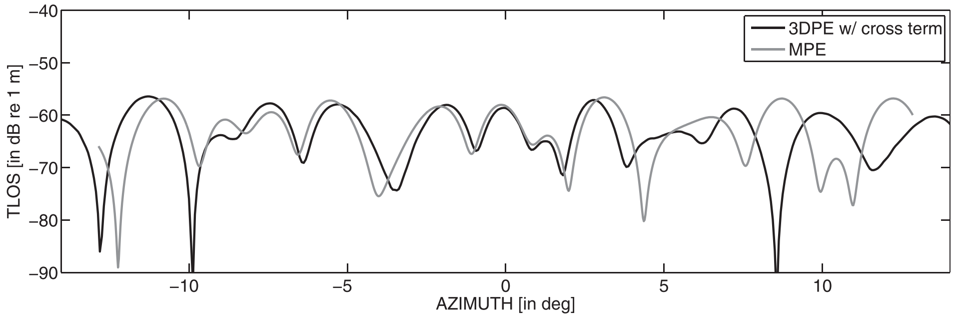

FIG. 4. Transmission loss (in dB re 1 m) curves at a fixed receiver depth of 10 m and a fixed receiver range of 8 km corresponding to the 3DPE solution (black curve) and the MPE solution (gray curve).

without step 3. The use of any higher-order approximation in depth and/or in azimuth did not modify the PE solutions (results not shown here). Also plotted in each subplot of Fig. 2 is the MPE analytical solution (14) with modal amplitudes computed using the analytical formula (18). From Fig. 2, one can notice the remarkable accuracy of the analytical solution. In particular, one can observe that the analytical solution takes into account the horizontal refraction effects which cannot be accurately reproduced by the 3D PE computation without cross terms.[4] Only the incorporation of a leading-order cross term (as proposed in Ref. 13) allowed us to achieve a good agreement between the analytical solution proposed here and the 3D PE numerical solution.

These comparisons show that the MPEs can handle horizontal refraction in the presence of bottom relief inhomogeneities very accurately. However, the mode coupling effects may cripple the accuracy of the adiabatic MPEs. This can be observed in our case by comparing the MPE solution with the 3D PE solution sufficiently far from the 90 m isobath, as shown in Fig. 3 (horizontal slices of transmission loss fields at a fixed depth of 10 m) and in Fig. 4 (transmission loss-versus-azimuth curves at a fixed range of 8 km and a fixed depth of 10 m, i.e., along the circular arc indicated by a black dashed line on each subplot of Fig. 3). While the contour plots in Fig. 3 seem very similar (at least in the far field, i.e., sufficiently far from the source), a closer inspection provided by Fig. 4 shows that the two solutions manifest (at a range of 8 km and a depth of 10 m) significant discrepancies for $\theta > 5^\circ$ and for $\theta < -10^\circ$. We can observe also that the inaccuracy of the MPE solution is more pronounced in the shallower part of the wedge-shaped waveguide. This deterioration is caused by the cutoff of the fourth mode at $y \approx -1.2$ km. Note that, following the discussion and results of Appendix C, the inaccuracy of the MPE for large θ cannot be attributed to the poor handling of horizontal refraction effects caused by the aperture limitation in the MPEs.

We again point out that the adiabatic MPE solution (14) proposed in this work is an analytical but asymptotic solution. The domain in the x,y horizontal plane where this asymptotic solution is sufficiently accurate can be arbitrarily large provided that the wedge angle is sufficiently small. In addition, the analytical solution is very easy to implement, does not demand large computational resources, and could thus be useful easily for comparisons with other more complex general-purpose 3D propagation models. A simple code that was used to produce the MPE solution figures of the present work ran in 4 s on an average personal computer (PC). For comparisons, the algorithm of Deane and Buckingham[8] for our test case took ~50 h to converge on the same computer. It is also important to note that the comparisons presented here are the first validation of the MPE theory (at least, to our knowledge) in the case of noncompact bottom inhomogeneities (the comparison in the case of the seamount was presented in Ref. 12).

VI. CONCLUSION

In this study, a new asymptotic analytical solution for the problem of wave propagation in a 3D penetrable wedge with a small apex angle was presented. The solution is based on the adiabatic MPE theory, and the solution of MPEs was analytically derived using operator disentanglement identities. The resulting formula for the acoustical field in the wedge-shaped waveguide was compared with the numerical solution of a fully 3D PE based model that includes a leading-order cross term correction, and a very good agreement was observed in the across-slope direction. Note that cross terms are introduced in 3D PE models in order to reduce the phase errors inherent to any 3D PE computation.

The necessity to incorporate cross terms in 3D PE models had already been demonstrated by Lin *et al.* a few years ago.[26] In their formulation, a series of higher-order cross terms was incorporated in a split-step Padé 3D PE algorithm written in Cartesian coordinates, and validated on the now very classical 3D ASA wedge benchmark problem. It was shown also very recently that a leading-order cross term correction can be sufficient to remove phase errors in 3D solutions obtained by 3D PE computations performed in cylindrical coordinates.[13] This approach was validated on the 3D ASA wedge benchmark. Note that the wedge angle for that specific test case is 2.86 deg, which is larger than the slope angle (0.5 deg) of the wedge-like test case considered in the present work. When comparisons of the adiabatic MPE analytical solution (14) with 3D PE solutions were initiated, it was unclear whether any cross term correction was needed or not. Interestingly, the comparisons shown in this study reveal that, even for a small wedge angle of 0.5 deg, a leading-order cross term correction is still required, which confirms the importance (at least, for benchmark comparisons) of incorporating cross-multiplied operator terms in 3D PE based computations.

Our analytical solution is valid only under the usual requirement of adiabatic theory, and there always exist some combinations of waveguide parameters for which it is inapplicable (e.g., when the source is located close to the cut-off depth of a mode). However, the adiabatic MPE analytical solution reported here is interesting for its explicit form; in particular, it shows what actually happens with normal modes when the bottom is slightly tilted [the behaviour of mode amplitudes subjected to horizontal refraction is clear from Eq. (18)]. By contrast, the existing solution of Deane and Buckingham,[8] although not restricted to the adiabatic case, has, however, a rather complicated form and provides no direct understanding of horizontal refraction effects. Furthermore, it is much more difficult to implement[29] and its computation can be very time consuming (in fact, for any specific case it is difficult to predict how many terms in the Bessel series are required to reach the convergence, not to mention the evaluation of the improper integral[8]). On the contrary, our analytical solution is very easy to implement, and its computation takes only a few seconds.[28] Thus, it can be useful when comparing with more complicated propagation models. In our opinion, it is also interesting from the purely academic point of view.

We also note that our approach may be used to obtain analytical solutions for a wide class of problems where mode coupling is relatively weak and MPEs admit analytical solution (see the classical paper of Weinberg and Burridge[18] for further details).

Finally, our work presents the first comparison of the adiabatic MPE solution with the results obtained by another method in the case of sloping bottom. Although the MPEs were introduced more than 20 years ago, to our knowledge, no comprehensive study of their validity was reported until now. Our results show that MPEs correctly handle bottom relief variations when no cutoff occurs.

ACKNOWLEDGMENTS

The work of P.S.P. was supported by the Russian Foundation for Basic Research foundation under Contracts Nos. 14-05-3148614_mol_a and 16-05-01074_a, the research program "Nonlinear dynamical processes in the ocean and atmosphere," of the V.I.Il'ichev Pacific Oceanological Institute and the Russian Federation President Grant No. MK-4323.2015.5. The authors express their gratitude to Professor S. V. Prants and Professor A. P. Kiselev for useful advice and comments.

APPENDIX A: DERIVATION OF THE SOLUTION TO MPES

A very elegant way to derive the analytical formula (18) is based on the various disentanglement identities from noncommutative analysis.[24]

The solution of the MPE (16) satisfying the initial condition $A_j(x,y)|_{x=0} = A_{j,0}(y)$ can be expressed in the form of operator exponent

$$A_j(x,y) = \mathrm{e}^{\mathrm{i}H_j x} A_{j,0}(y), \tag{A1}$$

where the Hamiltonian $H_j = (1/2k_j)(\partial_y^2 + b_j y + a_j)$. We recast Eq. (A1) in the form

$$A_j(x,y) = \mathrm{e}^{\mathrm{i}a_j x/(2k_j)} \mathrm{e}^{A+B} A_{j,0}(y).$$

In order to evaluate this expression, we must disentangle the operators $A = (\mathrm{i}x/2k_j)(\partial^2/\partial y^2)$ and $B = (\mathrm{i}x/2k_j)b_j y$ in the exponential e^{A+B}. This may be accomplished since A and B span a nilpotent Lie algebra.[24] The latter fact may be easily proved by explicit verification of the following commutation relations:

$$[A,B] = m\sqrt{A}\,,$$

$$[[A,B],B] = m^2/2\,,$$

$$[A,[A,B]] = 0\,,$$

where $m = b_j(\mathrm{i}x/(2k_j))^{3/2}$ (all commutators of higher order vanish).

The exponentials containing the operators that span nilpotent algebras may be disentangled by the Baker–Campbell–Hausdorff formula,[24] which expresses $\log(\mathrm{e}^X\mathrm{e}^Y)$ in terms of commutators of X and Y,

$$\log(\mathrm{e}^X\mathrm{e}^Y) = X + Y + \frac{1}{2}[X,Y] + \frac{1}{12}[X,[X,Y]] + \frac{1}{12}[[X,Y],Y] + \cdots. \tag{A2}$$

We write a simple identity

$$\mathrm{e}^{A+B} = \mathrm{e}^{\log(\mathrm{e}^{A+B}\mathrm{e}^{-B})}\mathrm{e}^B$$

and apply Eq. (A2) to $\log(\mathrm{e}^{A+B}\mathrm{e}^{-B})$ (i.e., $X = A+B$, $Y = -B$). After some algebra, we arrive at the following important formula:

$$\mathrm{e}^{A+B} = \mathrm{e}^{A-(m/2)\sqrt{A}+(m^2/12)}\mathrm{e}^B. \tag{A3}$$

In our case, it is essential to swap the expressions containing A and B. To do that, we derive here some nice commutation formulas. More precisely, we prove that if $[A,B] = m\sqrt{A}$, then

$$\mathrm{e}^A\mathrm{e}^B = \mathrm{e}^B\mathrm{e}^A\mathrm{e}^{m\sqrt{A}+m^2/4}. \tag{A4}$$

The proof consists in the evaluation of

$$[\mathrm{e}^A,\mathrm{e}^B] = \mathrm{e}^{-A}\mathrm{e}^{-B}\mathrm{e}^A\mathrm{e}^B = \mathrm{e}^{-P}\mathrm{e}^Q,$$

where we introduced notation $Q = \log(\mathrm{e}^A\mathrm{e}^B), -P = -\log(\mathrm{e}^A\mathrm{e}^B) = \log(\mathrm{e}^{-A}\mathrm{e}^{-B})$. Operators P and Q may be computed straightforwardly using formula (A2),

$$Q = A + B + \frac{1}{2}[A,B] + \frac{1}{12}[A,[A,B]] + \frac{1}{12}[[A,B],B],$$

$$P = B + A + \frac{1}{2}[B,A] + \frac{1}{12}[B,[B,A]] + \frac{1}{12}[[B,A],A].$$

Now we notice that

$$[\mathrm{e}^A,\mathrm{e}^B] = \exp(\log(\mathrm{e}^{-P}\mathrm{e}^Q))$$

and apply Eq. (A2) again, this time to $\log(\mathrm{e}^{-P}\mathrm{e}^Q)$. After some simple transformations, we obtain

$$[\mathrm{e}^A, \mathrm{e}^B] = \mathrm{e}^{m\sqrt{A}+m^2/4}.$$

It is even easier to show that for operators P and Q satisfying relation $[P, Q] = r$, we have

$$\mathrm{e}^P \mathrm{e}^Q = \mathrm{e}^Q \mathrm{e}^P \mathrm{e}^r.$$

This allows us to swap B and $\sqrt{A}$ in Eq. (A3). Using this formula and Eq. (A4), we obtain (after two swaps) the final expression for disentangled exponentials

$$\mathrm{e}^{A+B} = \mathrm{e}^{B+(m^2/12)} \mathrm{e}^{(m/2)\sqrt{A}} \mathrm{e}^A. \tag{A5}$$

Note that e^A is a convolution operator with the Green function of the free-particle Schrödinger equation as its kernel[25]

$$\mathrm{e}^{q(\partial^2/\partial y^2)} g(y) = \frac{1}{2\sqrt{\pi q}} \int_{-\infty}^{\infty} \mathrm{e}^{-\left[(y-\xi)^2/4q\right]} g(\xi)\, \mathrm{d}\xi. \tag{A6}$$

In particular, in the case of a Gaussian function $g(y) = \mathrm{e}^{-y^2/\sigma^2}$, the integral in Eq. (A6) may be evaluated explicitly

$$\begin{aligned} \mathrm{e}^{q(\partial^2/\partial y^2)} \mathrm{e}^{-y^2/\sigma^2} &= \frac{1}{2\sqrt{\pi q}} \int_{-\infty}^{\infty} \mathrm{e}^{-\left[(y-\xi)^2/4q\right]} \mathrm{e}^{-\xi^2/\sigma^2}\, \mathrm{d}\xi \\ &= \sqrt{\frac{\sigma^2}{\sigma^2+4q}} \mathrm{e}^{-y^2/\sigma^2+4q}. \end{aligned} \tag{A7}$$

Also note that $\sqrt{\mathrm{A}}$ is merely a shift operator

$$\mathrm{e}^{q(\partial/\partial y)} g(y) = g(y+q). \tag{A8}$$

Now we have all the formulas we need for the evaluation of $\mathrm{e}^{\mathrm{i}H_j x} A_{j,0}(y)$ for the Gaussian initial condition $A_{j,0}(y) = \bar{A}_j\, \mathrm{e}^{-k_j^2 y^2}$. First, we use the convenient disentanglement identity (A5), next we apply operators on the right-hand side one by one, using Eqs. (A7) and (A8). Finally, after some simple transformations, we arrive at Eq. (A8).

APPENDIX B: DERIVATION OF THE GAUSSIAN STARTER PARAMETERS

In this appendix, we derive the formulas for the parameters of the Gaussian starter (13) for the MPE (12). Note that our derivation is similar to the derivation of the classical Gaussian source for the 2D narrow-angle PE.[1] Let $1 \le j \le N_m$. A general form of the Gaussian initial condition can be written as

$$A_j(x, y)|_{x=0} = \bar{A}_j\, \mathrm{e}^{-y^2/w_j^2}, \tag{B1}$$

where the two parameters $\overline{A_j}$ and w_j are to be determined.

Consider a single-mode partial solution of the homogeneous Helmholtz equation[1] in a homogeneous medium with a flat bottom at $z = h_0$,

$$p_j(x, y, z) = \frac{\mathrm{i}}{4\rho_w} \phi_j(z_s) H_0^{(1)}(k_j r) \phi_j(z), \tag{B2}$$

where $r = \sqrt{x^2+y^2}$. For this waveguide, the adiabatic MPE (12) can be written as

$$2\mathrm{i}k_j \partial_x A_j + \partial_y^2 A_j = 0. \tag{B3}$$

The solution of Eq. (B3) satisfying the initial condition (B1) is written as[1]

$$A_j(x, y) = \frac{\bar{A}_j}{\sqrt{1+\dfrac{2\mathrm{i}x}{k_j w_j^2}}} \exp\left(-\frac{y^2}{w_j^2\left(1+\dfrac{2\mathrm{i}x}{k_j w_j^2}\right)}\right), \tag{B4}$$

and the adiabatic MPE approximation for the single-mode solution denoted $\bar{p}_j$ thus reads

$$\bar{p}_j(x, y, z) = A_j(x, y) \mathrm{e}^{\mathrm{i}k_j x} \phi_j(z). \tag{B5}$$

Parameters w_j and $\bar{A}_j$ are now determined by matching the first-order terms of the asymptotic expansions of Eqs. (B5) and (B2) in the far field. More precisely, we evaluate first the squared magnitudes of complex quantities (B5) and (B2), applying the far-field approximation for the Hankel function in Eq. (B2),

$$|p_j(x, y, z)|^2 \approx \frac{\phi_j(z_s)^2 \phi_j(z)^2}{8\pi k_j \rho_w^2 x \sqrt{1+\left(\dfrac{y}{x}\right)^2}}.$$

We also drop higher-order terms in x in the expression of the squared magnitude of $\bar{p}_j$,

$$\begin{aligned} |\bar{p}_j(x,y,z)|^2 &= \frac{\bar{A}_j^2}{\sqrt{1+\dfrac{4x^2}{k_j^2 w_j^4}}} \exp\left(-\frac{2y^2}{w_j^2\left(1+\dfrac{4x^2}{k_j^2 w_j^4}\right)}\right) \phi_j(z)^2 \\ &\approx \frac{k_j w_j^2 \bar{A}_j^2}{2x} \exp\left(-\frac{k_j^2 w_j^2}{2}\left(\frac{y}{x}\right)^2\right) \phi_j(z)^2. \end{aligned}$$

We then make power series expansions of the above expressions for $|\bar{p}_j|^2$ and $|p_j|^2$ with respect to $y\,/\,x$ about $y/x = 0$ (thus, taking into account only waves propagating at small angles with respect to the line $y = 0$). By retaining only terms up to second order in $y\,/\,x$, we obtain

$$|p_j(x, y, z)|^2 \approx \frac{\phi_j(z_s)^2 \phi_j(z)^2}{8\pi k_j \rho_w^2 x} \left(1 - \frac{1}{2}\left(\frac{y}{x}\right)^2\right),$$

$$|\bar{p}_j(x, y, z)|^2 \approx \frac{k_j w_j^2 \bar{A}_j^2 \phi_j(z)^2}{2x} \left(1 - \frac{k_j^2 w_j^2}{2}\left(\frac{y}{x}\right)^2\right).$$

By comparing these two equations, we conclude that a field matching can be achieved by selecting the following values for $\bar{A}_j$ and w_j:

$$w_j = \frac{1}{k_j}, \quad \bar{A}_j = \frac{\phi_j(z_s)}{2\sqrt{\pi}\rho_w}. \tag{B6}$$

APPENDIX C: MPE SOLUTION IN ROTATED COORDINATES

In this appendix, we briefly discuss what happens if we write the adiabatic MPE in a horizontal coordinate system rotated by an angle θ about the z axis (i.e., when the y axis is aligned at an angle θ with respect to the wedge apex). In this case, the adiabatic MPE (12) can be rewritten as

$$2\mathrm{i}k_j\partial_x A_j + \partial_y^2 A_j + (b_j y + d_j x + a_j)A_j = 0, \tag{C1}$$

where $b_j = \tan(\alpha)\cos(\theta)B_{jj}$, $d_j = \tan(\alpha)\sin(\theta)B_{jj}$, and a_j is given by Eq. (17).

The Cauchy problem for Eq. (C1) in the halfspace $x \geq 0$ with initial condition (13) has the following solution:

$$A_j(x,y) = \bar{A}_j\sqrt{\frac{1}{1+2\mathrm{i}k_j x}}\exp\left(\frac{2\mathrm{i}a_j x + \mathrm{i}d_j x^2}{4k_j} + \frac{\mathrm{i}b_j yx}{2k_j} - \frac{\mathrm{i}x^3 b_j^2}{24k_j^3}\right)\exp\left(-\frac{\left(yk_j - \dfrac{x^2 b_j}{4k_j}\right)^2}{1+2\mathrm{i}k_j x}\right). \tag{C2}$$

Clearly, formula (C2) reduces to Eq. (18) when $\theta = 0$. It is easy to see that the derivation Eq. (C2) is accomplished following the same steps as described in Appendix A (the additional term that appears in the first operator exponential does not produce any problem since it commutes with operators A and B).

It is now natural to obtain a solution of the wedge problem solving the MPEs (C1) along the fan of rays starting at the source. More precisely, for each point (x,y) we can compute the pressure $P(x,y,z)$ using the MPE solution (C2) along the ray passing through (x,y), i.e., using $\theta = \mathrm{atan}(y/x)$. It turned out, however, that such a solution did not provide any improvement in accuracy for large $|y|$. This indicates that the accuracy of the adiabatic MPE in our case is not limited by the narrow-angle approximation made when Eq. (11) is replaced by Eq. (12). Rather, the limitation is imposed by neglecting mode interaction when coupling terms in Eq. (10) were dropped.

[1]F. B. Jensen, W. Kuperman, M. Porter, and H. Schmidt, *Computational Ocean Acoustics* (Springer, New-York, 2000).

[2]A. Tolstoy, "3-D propagation issues and models," J. Comput. Acoust. **4**, 243–271 (1996).

[3]E. Westwood, "Complex ray solutions to the 3-D wedge ASA benchmark problems," J. Acoust. Soc. Am. **109**, 2333 (2001).

[4]F. Sturm, "Numerical study of broadband sound pulse propagation in three-dimensional oceanic waveguides," J. Acoust. Soc. Am. **117**, 1058–1079 (2005).

[5]P. Borejko, "An analysis of cross-slope pulse propagation in a shallow water wedge," in *Proceedings of the 10th Conference on Underwater Acoustics*, edited by T. Akal, Istanbul, Turkey (2010).

[6]V. M. Babich, N. V. Mokeeva, and B. A. Samokish, "The problem of scattering of a plane wave by a transparent wedge: A computational approach," J. Commun. Technol. Electron. **57**, 993–1000 (2012).

[7]J.-P. Croisille and G. Lebeau, *Diffraction by an Immersed Elastic Wedge* (Springer, New York, 1999).

[8]G. B. Deane and M. J. Buckingham, "An analysis of the three-dimensional sound field in a penetrable wedge with a stratified fluid or elastic basement," J. Acoust. Soc. Am. **93**, 1319–1328 (1993).

[9]M. D. Collins, "The adiabatic mode parabolic equation," J. Acoust. Soc. Am. **94**, 2269–2278 (1993).

[10]A. T. Abawi, W. A. Kuperman, and M. D. Collins, "The coupled mode parabolic equation," J. Acoust. Soc. Am. **102**, 233–238 (1997).

[11]M. Y. Trofimov, "Narrow-angle parabolic equations of adiabatic single-mode propagation in horizontally inhomogeneous shallow sea," Acoust. Phys. **45**, 575–580 (1999).

[12]P. S. Petrov, M. Y. Trofimov, and A. D. Zakharenko, "Mode parabolic equations for the modeling of sound propagation in 3D-varying shallow water waveguides," in *Proc. Intern. Conf. "Days on Diffraction 2012"* (2012).

[13]F. Sturm, "Leading-order cross term correction of three-dimensional parabolic equation models," J. Acoust. Soc. Am. **139**, 263–270 (2016).

[14]P. S. Petrov and T. N. Petrova, "Asymptotic solution for the problem of sound propagation in a sea with an underwater canyon," J. Acoust. Soc. Am. **136**, EL281–EL287 (2014).

[15]A. D. Pierce, "Extension of the method of normal modes to sound propagation in an almost stratified medium," J. Acoust. Soc. Am. **37**, 19–27 (1965).

[16]H. Weinberg and R. Burridge, "Horizontal ray theory for ocean acoustics," J. Acoust. Soc. Am. **55**, 63–79 (1974).

[17]G. V. Frisk, *Ocean and Seabed Acoustics: A Theory of Wave Propagation* (Prentice-Hall, Englewood Cliffs, NJ, 1994).

[18]J. Wei and E. Norman, "Lie algebraic solution of linear differential equations," J. Math. Phys. **4**, 575–581 (1963).

[19]S. V. Prants, "An algebraic approach to quadratic parametric processes," J. Phys. A: Math. Gen. **19**, 3457–3462 (1986).

[20]G. Dattoli, P. L. Ottaviani, A. Torre, and L. Vásquez, "Evolution operator equations: Integration with algebraic and finite-difference methods. Applications to physical problems in classical and quantum mechanics and quantum field theory," Riv. Nuovo Cimento **20**, 1–133 (1997).

[21]P. S. Petrov, "Asymptotic solution for the problem of acoustic waves propagation in a penetrable truncated wedge," in *Proc. Intern. Conf. "Days on Diffraction 2013"* (2013).

[22]A. Bamberger, B. Engquist, L. Halpern, and P. Joly, "Higher order paraxial wave equation approximations in heterogeneous media," SIAM J. Appl. Math. **48**, 129–154 (1988).

[23]M. D. Collins, "Higher order Padé approximations for accurate and stable elastic parabolic equations with application to interface wave propagation," J. Acoust. Soc. Am. **89**, 1050–1057 (1991).

[24]V. E. Nazaikinskii, V. Shatalov, and B. Y. Sternin, *Methods of Noncommutative Analysis. Theory and Applications* (Walter de Gruyter, Berlin, 1996).

[25]R. D. Richtmyer, *Principles of Advanced Mathematical Physics* (Springer, New York, 1978).

[26]Y.-T. Lin, J. M. Collis, and T. F. Duda, "A three-dimensional parabolic equation model of sound propagation using higher-order operator splitting and Padé approximants," J. Acoust. Soc. Am. **132**, EL364–EL370 (2012).

[27]Note that use the sum of $\phi_j(z)$ computed at $y = 0$ rather then the combination of $\phi_j(z,y)$ used in Refs. 9 and 10, since the bottom relief is taken into account via the modified interface conditions as shown in Ref. 14, and references therein.

[28]P. S. Petrov, "MPE solution for a 3D wedge (MATLAB code)" (2015), available at http://oalib.hlsresearch.com/ThreeD/Petrov/MPE_wedge_solution%202/ (Last viewed 19 September 2015).

[29]P. S. Petrov, "The 3D penetrable wedge solution of G. Deane and M. Buckingham (MATLAB code)" (2015), available at http://oalib.hlsresearch.com/ThreeD/Petrov/PenetrableWedge/ (Last viewed 19 September 2015).